СООБЩЕНИЯ
ОБЪЕДИНЕННОГО
ИНСТИТУТА
ЯДЕРНЫХ
ИССЛЕДОВАНИЙ
ДУБНА



E4 - 6895

R.A.Eramzhyan, H.U.Jäger , H.R.Kissener

# ON THE DECAY OF THE PHOTO RESONANCE IN $^{14}$N AND $^{14}$C NUCLEI

1973

ЛАБОРАТОРИЯ
ТЕОРЕТИЧЕСКОЙ ФИЗИКИ

E4 - 6895

R.A.Eramzhyan, H.U.Jäger*, H.R.Kissener*

# ON THE DECAY OF THE PHOTO RESONANCE IN $^{14}N$ AND $^{14}C$ NUCLEI

* Zentralinstitut für Kernforschung, Bereich 2, Rossendorf bei Dresden, DDR

Эрамжян Р.А., Егер Г.-У., Киссенер Г.-Р.

E4 - 6395

Распад состояний гигантского резонанса фотопоглощения в ядрах $^{14}N$ и $^{14}C$

Рассмотрен распад состояний гигантского резонанса фотопоглощения в ядрах $^{14}N$ и $^{14}C$ в рамках модели оболочек с учетом корреляций нуклонов в ядре. Рассчитаны сечения переходов на отдельные состояния конечного ядра. Проведено сравнение с экспериментальными данными.

Сообщение Объединенного института ядерных исследований
Дубна, 1973

Eramzhyan R.A., Jäger H.U., Kissener H.R.

E4 - 6895

On the Decay of the Photo Resonance in $^{14}N$ and $^{14}C$ Nuclei

The decay of the photo resonances in $^{14}N$ and $^{14}C$ nuclei is analyzed in terms of the shell model with intermediate coupling. Cross-sections and branching ratios of nucleon channels are compared with experimental data. Successive decay branches are estimated.

Communications of the Joint Institute for Nuclear Research.
Dubna, 1973

## I. Introduction

It became clear in the last decade that the gross structure of photo absorption curves in light nuclei (position and width of the main maximum, configurational and isospin splitting) can be well understood on the basis of the shell model if one takes into account the residual interaction between the nucleons. Now the interest has moved to new features of the giant resonance (which are not seen by measuring only total cross-sections) as the intermediate structure, the decay modes, the branching ratios to definite final states of the residual nuclei, the angular and energy distributions of outgoing particles, etc. Such data provide also more thorough tests of model descriptions, and at present there is much activity in the detailed investigation of this field, both experimentally and theoretically.

We have extended our previous shell model analysis of non-normal parity spectra and photo absorption for 1p shell nuclei[1] to the decay of the photo resonance. In this paper we consider the nuclei $^{14}N$ and $^{14}C$ and compare the results with existing data, in particular with recently measured partial $(\gamma, p)$ and $(\gamma,n)$ cross-sections. We have included the secondary decay $^{13}C(N) \rightarrow ^{12}C + n(p)$ in order to determine total $(\gamma,p)$, $(\gamma,n)$, $(\gamma,pn)$ and the $^{14}N(\gamma,pn\,3\alpha)$ cross-sections which almost exhaust the total absorption.

Particular attention is devoted to the $^{14}N$ case since for this nucleus rich experimental information is available. From

this example we hope to learn about the range of application of this model to other 1p nuclei. A particular feature of the photo absorption cross-sections of nuclei with N≠Z (the isospin splitting of the giant resonance) is illustrated by the $^{14}C$ nucleus.

## 2. Details of the Calculation

Our calculation involves non-spurious bound-state shell-model wave functions with pure isospin, obtained by diagonalizing an effective Hamiltonian which contains Cohen-Kurath 1p-shell matrix elements[2] and Gillet's interaction "CAL"[3] between nucleons in different shells. The configurational space has been restricted to all $1\hbar\omega$ excitations of A=14 nucleons in the oscillator orbits N=0,1 and 2. The decay branches and nucleon widths of the excited states have been calculated following the R matrix formulation[4]. The expression used for the partial nucleon width is

$$\Gamma_{i\to f} = 2k\gamma_0^2 \sum_\ell P_\ell S_\ell \quad , \quad \text{with} \quad \gamma_0^2 \simeq \hbar^2/\mu a_c \quad ,$$

where $k$ is the wave number of the relative motion in the final channel; $P_l$ and $S_l$ are the penetration and spectroscopic factors for emission of a nucleon with orbital angular momentum $l$; $\gamma_0^2$ is the reduced one-particle width, $\mu$ is the reduced mass, and $a_c$ is the channel radius. The corresponding branch of the integrated photo absorption cross-section is

$$\sigma_{i\to f} = \sigma_i \Gamma_{i\to f} / \Gamma_i \quad , \quad \sigma_i = \int_{line} \sigma_\gamma (g.s. \to i)\, dE$$

with $\Gamma_i$ being the total width of level i. The decay branches (in MeV.mb) have been converted to cross-sections by spreading



them over non-interfering Breit-Wigner curves of width $\Gamma_i$ at the proper energies.

The oscillator length has been put equal to 1.7 fm as is suggested by the scattering data of ref.[5]. The channel radius was taken as 4 fm.

## 3. Results and Discussion

### 3.1. The $^{14}N$ Photo Resonance

The total photo absorption curve of $^{14}N$ shows a rather smooth energy dependence as compared with other 1p shell nuclei. A recent measurement[6] (up to 30 MeV photon energy) shows a strong peak at 22.5 MeV and considerable tail at higher energies (see fig. 1). The calculated curve, in the energy range covered by this experiment, reflects the gross structure of the data, except for the absolute value of the cross-section (see table 1). According to the calculation the strongest absorption line corresponds to dominating $1p_{3/2} \to 1d_{5/2}$ excitation. A broad peak containing about 10 percent of the total strength appears above 40 MeV photon energy (see fig. 3) and corresponds to the excitation of a 1s nucleon into the 1p shell. Its position is strongly dependent on the choice of the 1s hole energy which could not be determined from the low-energy

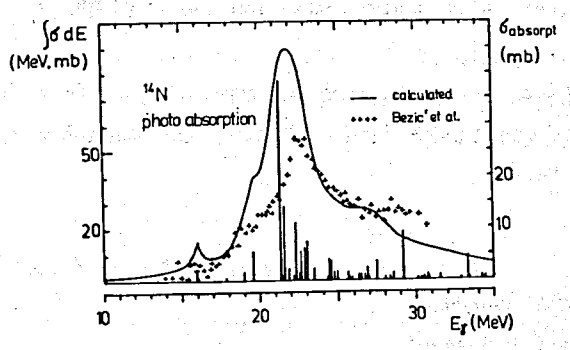


Fig. 1. Total photo absorption cross-section for $^{14}N$ nuclei. The experimental data are taken from ref.[6]. The vertical bars give the calculated integrated strength for E1 absorption (left scale). The solid line corresponds to the cross-section (right scale).



Table 1.

Integrated cross-sections for several photo reactions on $^{14}N$

| reaction | | ref. | endpoint. (MeV) | int.cross-sect. (MeV.mb) | % of integral absorption |
|---|---|---|---|---|---|
| photo absorpt. | exp. | 6) | 31 | 195±37 | |
| | | 14) | 90 | 330±20 | |
| | | 15) | 170 | 347 | |
| | present work | | 30 | 285 | |
| | | | total | 356 | |
| (γ, p) | exp. | 8) | 25 | | 21.5 |
| | | 12) | 30 | 26 | |
| | | 14) | 90 | 92 | 28 |
| | | 15) | 170 | 38 | 11 |
| | present work | | | 32 | 9.1 |
| (γ,n) | exp. | 11) | 25 | 15 | 12 |
| | | 14) | 90 | 53 | 16 |
| | | 15) | 170 | 31 | 9 |
| | present work | | | 16 | 4.6 |
| (γ,pn) | exp. | 12) | 29 | 43 | |
| | | 14) | 90 | 116 | 35 |
| | | 15) | 170 | 128 | 37 |
| | present work | | | 286 | 80.5 |
| (γ,pn3α) | exp. | 14) | 90 | 36 | 11 |
| | present work | | | 21 | 5.8 |

spectra but has been fixed to $\mathcal{E}_{1s'} = -27.5$ MeV.*

The calculated curve in fig.1 refers to electric dipole absorption. A notable contribution of M1 strenght at $E_\gamma = 21.1$ MeV reported by Bentz[8] is not obtained using the Cohen-Kurath wave functions. The calculation yields however a remarkable M1 absorption (2 MeV.mb) to $2^+$, T=1 levels around $E_\gamma \simeq 10$ MeV. This intensity may be splitted among the two neighbouring $2^+$,1 levels at 9.17 and 10.43 MeV which are also strongly excited in M1 electron scattering[7].

There exists a bulk of data on the decay of photo resonance in $^{14}N$. In most of the experiments bremsstrahlung photons at various endpoint energies have been used. Cross-sections for the groundstate transitions $(\gamma, p_o)$ and $(\gamma, n_o)$ have been reported by Wahlström[9], Kosiek[10], King[11], Bentz[8] and Gellie[20]. The cross-sections for the decay to excited states of $A$ =13 nuclei have been determined by Thompson[12], Bentz[8] and Gellie[20] (see tables 1 and 2). The inverse reactions $^{13}C(p, \gamma_{0,1})$ have been studied by Riess et al.[21] for proton energies covering the $^{14}N$ giant resonance. The total $(\gamma, n)$ cross-section was measured by Berman[13]. Further, many cross-sections of reactions with charged particles in the exit channel have been determined by Komar[14] and Gorbu -

*There is a slight difference between the calculated absorption curves in this paper and in a previous one 1 . This is partly due to the smoothing procedure applied here and to the use of calculated widths instead of arbitrary ones and partly due to an error in our first calculation where the matrix elements $\langle 1s, (2s, 1d) | V | (1p)^2 \rangle$ had been taken with the wrong sign. These matrix elements couple the basic states of the two configurations $(1s)^{-1}(1p)^{A-3}$ and $(1s)^4 (1p)^{A-5}(2s,1d)^1$. Repeating the calculation with the correct 1s phase, the low-energy spectra and the photo absorption cross-section up to 30 MeV remained almost unchanged. States with dominant 1s hole structure are however notable affected and give rise to the above-mentioned high-energy peak.



Table 2.

Branching ratios and integrated cross-sections for the decay of the $^{14}N$ photo resonance to particular final states. The relative values (in %) refer to the integral photo absorption cross-section

| | final J | state E(MeV) | integr.cross-sect. (MeV.mb) exp. | (mostly ref.8) | pres. work | branching (%) exp. | (mostly ref.8) | calculated ref. 16) | present work |
|---|---|---|---|---|---|---|---|---|---|
| $^{13}C$ | $1/2^-$ | g.s. | 15 | | 19(E1) | ≈15 | | 7.8 | 5.3 |
| | | | 18.5±4[a] | | 2(M1) | | | | |
| | $3/2^-$ | 3.68 | 6 | | 13 | ≈5.5 | | 14.5 | 3.8 |
| | | | 7 ± 2[b] | | | | | | |
| | $5/2^-$ | 7.55 | 15; 17[e] | | 63 | ≈15 | | 12.8 | 18 |
| | $1/2$ | 8.86 | | | 20 | | | 9.8 | 5.8 |
| | $3/2^-$ | 9.52 | >3 | | | >3 | | | |
| | | 9.90 | | | 26 | | | | 7.5 |
| | $3/2^-$ | 11.72 | >5 | | 8 | >5.5 | | 4.8 | 2.4 |
| $^{13}N$ | $1/2^-$ | g.s. | 15[c]; 20[e] | | 16 | 16 | | 4.9 | 4.6 |
| | $3/2^-$ | 3.51 | 6[e] | | 11 | 5.5 | | 10.8 | 3.2 |
| | $5/2^-$ | 7.39 | | | 40 | | | 10.4 | 11.6 |
| | $1/2^-$ | 8.91 | | | 12 | ≈25 | | 8.1 | 3.4 |
| | $3/2^-$ | 9.52 | | | 13 | | | | 3.8 |
| $^{12}C$ | $0^+$ | g.s. | | | 158 | 44.5 | | | 44 |
| | $2^+$ | 4.44 | 23±6[b] | | 128 | 18 | | | 35 |
| | $\alpha$-instable levels | | 36[d] | | 21 | 11[d] | | | 5.8 |

a) ref. 9)
b) ref. 12)
c) ref. 11)
d) ref. 14)
e) ref. 20)

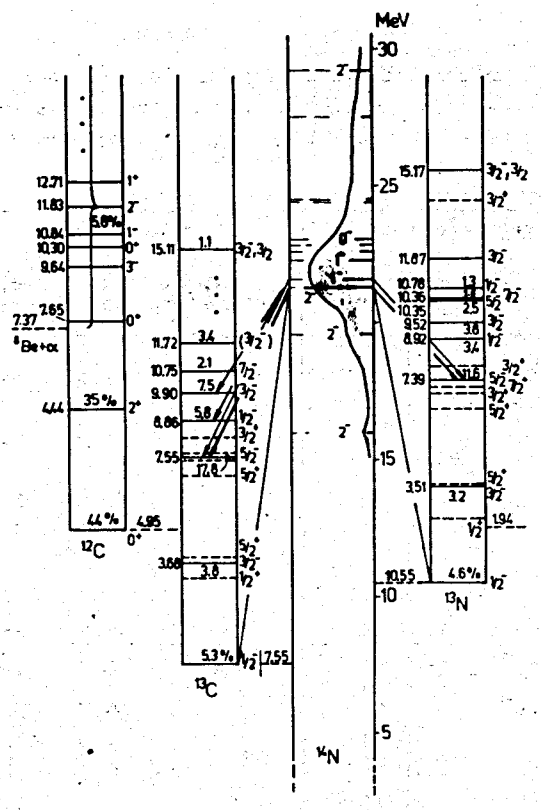


Fig. 2. Energy scales and residual state population in the decay of the $^{14}N$ photo resonance. Spin and absorption strength for the dominating dipole states are indicated. The weakly populated non-normal parity levels of $^{13}C$ and $^{13}N$ are shown by dashed lines. The calculated level population is given in percent of the total absorption. Q values in MeV for some photo reactions are: $(\gamma,p)$ 7.55; $(\gamma,d)$ 10.27; $(\gamma,n)$ 10.55; $(\gamma,\alpha)$ 11.61; $(\gamma,pn)$ 12.49; $(\gamma,2\alpha)$ 16.06; $(\gamma,p\alpha)$ 18.20; $(\gamma,pn3\alpha)$ 19.77; $(\gamma,n\alpha)$ 20.05; $(\gamma,2p)$ 25.08; $(\gamma,2n)$ 30.64.



nov[15], using the cloud chamber technique. In the region of the main absorption peak many decay channels are energetically possible (see caption to fig.2). The $(\gamma,d)$, $(\gamma,\alpha)$ and $(\gamma,2\alpha)$ reactions to the T=0 levels of the residual nuclei are isospin-forbidden. Experimentally the $(\gamma,\alpha)$ branch is 2% of the total absorption rate[14,15], and the $(\gamma,d)$ yield was found to be two orders of magnitude lower than the $(\gamma,p)$ yield[15]. The $(\gamma,pn\,3\alpha)$ channel is the most important one among the $\alpha$ decay modes. The relative yield of $\alpha$-producing reactions suggests that the $\alpha$ emission proceeds preferably after sequential nucleon decays to highly excited levels of the $^{12}C$ nucleus. Some experimental integrated cross-sections and the calculated results are compiled in table 1. The total $(\gamma,n)$ and $(\gamma,pn)$ cross-sections and the branches to definite levels in $^{12}C$ are estimated by taking into account only successive primary and secondary nucleon emission. Other decay channels have been neglected because of their high Q values.

Figure 2 shows the energy scales involved in the photo reactions on $^{14}N$ and the calculated population of low-lying levels in the neighbouring residual nuclei. Comparing the decay to mirror levels of the A=13 nuclei we note approximate symmetry between the primary p and n channels which receive 60 and 40 percent of the total strength. The difference of penetrability for p and n emission is slightly overcompensated by the difference of the Q values. The primary decay proceeds mainly to levels in $^{13}C$ and $^{13}N$ with ground state parity. Levels with opposite parity are only weakly populated; the calculation yields 5% of the total strength. Among the normal-parity

Table 3.

Calculated spectroscopic factors and cross-sections for the decay of the strongest dipole state in $^{14}N$ ($2^-$, T=1, 22 MeV, 78 MeV.mb) to several final states in $^{13}C$ and $^{13}N$ nuclei

| final state J | E(MeV) $^{13}C$ | $^{13}N$ | emitted nucleon | spectroscop. factor | integr. sect. $^{13}C$ | cross-sect. (MeV.mb) $^{13}N$ |
|---|---|---|---|---|---|---|
| $1/2^-$ | g.s. | | $d_{5/2}$ | 0.002 | 0.9 | 0.9 |
| | | | $d_{3/2}$ | 0.020 | 8.0 | 7.3 |
| $3/2^-$ | 3.68 | 3.51 | $d_{5/2}$ | 0.002 | 0.7 | 0.6 |
| | | | $d_{3/2}$ | 0.005 | 1.3 | 1.1 |
| | | | 2s | 0.001 | 0.2 | 0.2 |
| $5/2^-$ | 7.55 | 7.40 | $d_{5/2}$ | 0.129 | 18.0 | 10.4 |
| | | | $d_{3/2}$ | 0.010 | 1.4 | 0.8 |
| | | | 2s | 0.015 | 5.2 | 4.5 |
| $1/2^-$ | 8.86 | 8.92 | $d_{5/2}$ | 0.033 | 3.1 | 1.2 |
| | | | $d_{3/2}$ | 0.035 | 3.3 | 1.3 |
| $3/2^-$ | 9.90 | 9.52 | $d_{5/2}$ | 0.164 | 5.0 | $\approx 0$ |
| | | | $d_{3/2}$ | 0.001 | $\approx 0$ | $\approx 0$ |
| | | | 2s | 0.002 | 0.5 | 0.2 |



levels in the A=13 nuclei only the ground-states and the first excited $3/2^-$, 3.68 MeV level in $^{13}C$ are stable against secondary nucleon decay to $^{12}C$. Hence, the main decay mode is the ($\gamma$,pn) channel. Important primary transitions are those to the first excited $5/2^-$ states and to the ground-states in $^{13}C$ and $^{13}N$ which is in qualitative agreement with the experimental data (see table 2). The calculated ground-state branches (in percent of the integral photo absorption) are considerably smaller than the experimental ratios. This is partly due to the fact that the experiment[8] extends only up to 25 MeV photon energy whereas the calculation includes the total absorption, and the high-energy tail of the photo resonance decays preferably into levels above 10 MeV excitation energy of the residual nuclei. The ratios of decay branches to several excited levels are in qualitative agreement with the experiment. In table 2 the results of a recent calculation by Goncharova[16], which has been performed on a more restricted basis than ours but leads to similar results, are included.

The selectivity of the decay is further illustrated in table 3 by giving some details on the branching of the strongest dipole state at 22 MeV. This state decays mainly by $l=2$ transfer as was confirmed by experiment[8]. From the structure of the wave functions the decay to the first $5/2^-$ and the second $3/2^-$ levels in the A=13 nuclei is clearly favoured over the transitions to the ground states and the first $3/2^-$ levels. The parentage relations are somewhat masked by the strong energy dependence of the barrier penetration.

Next we consider the enrgy dependence of partial cross-

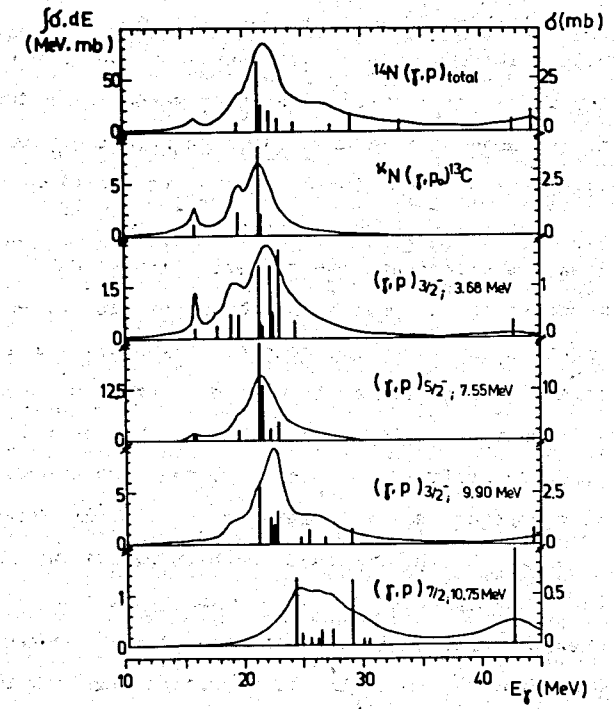


Fig. 3. Calculated cross-sections for the total and several partial ($\gamma$,p) reactions on $^{14}N$.



sections. Figure 3 displays our calculated cross-sections for proton decay to the lowest normal-parity levels in $^{13}C$. Up to about 10 MeV excitation energy the final states are mainly populated from the region around the giant resonance peak. Lavels above 10 MeV (e.g. the $7/2^-$ state at 10.75 MeV) are however preferable fed by the high-energy tail of the photo resonance. Figures 4 and 5 present the measured ($\gamma$,$p_o$) and ($\gamma$,$n_o$) cross-sections[8-11] together with the calculated ones. Figure 6 shows the corresponding curves for the ($\gamma$, $p_{3.68}$) reaction. In all three cases we note a satisfactory agreement between the data and the calculated cross-sections for both the position of the main maxima and the gross-structure of the curves. The narrow resonances in the ($\gamma$, $p_{3.68}$) reaction above 20 MeV can not of course be reproduced; the widths of the corresponding absorption lines are now comparable with their distances.

In fig.7 the total ($\gamma$,n) cross-section up to 29 MeV photon energy obtained by Berman et al.[13] is shown. For comparison an estimate of this cross-section including the secondary nucleon decay $^{13}C(N) \rightarrow ^{12}C$ is given. Other neutron-spending channels were neglected because of their Q values. Hence, we have as an upper limit

$$\sigma(\gamma,n)_{tot} \simeq \sigma_{abs.} - \sigma(\gamma,p_o) - \sigma(\gamma,p_{3.68}) \ .$$

The agreement with the experimental curve is good, apart from the absolute value of the cross-section.

The strongly populated $5/2^-$, 7.55 MeV level in $^{13}C$ is of particular interest. Its anomalous stability was first discussed by Balashov et al.[17]. In the adopted configurational space this level cannot decay to the $^{12}C$ ground-state because the tran-

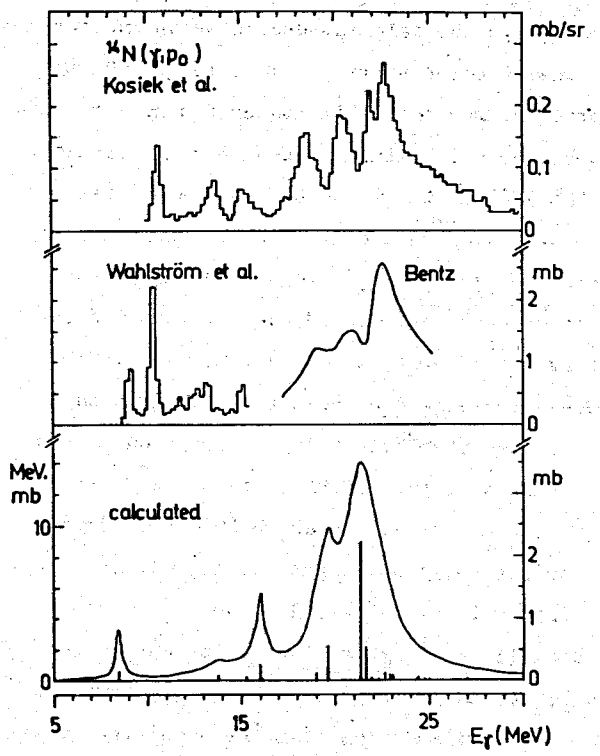


Fig. 4. Experimental and calculated $^{14}N(\gamma,p_0)^{13}C$ cross-sections. The experimental data are taken from refs.[8-10].



Fig. 5. Experimental and calculated $^{14}N(\gamma,n_0)^{13}N$ cross-sections. The experimental data are taken from ref.[11].

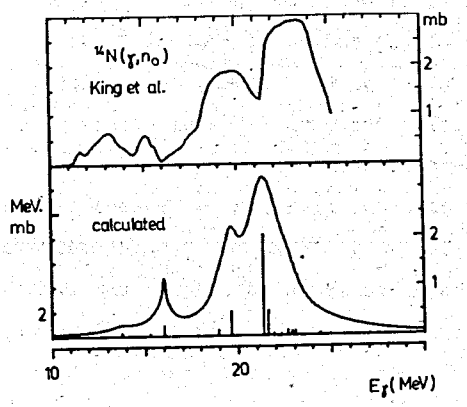


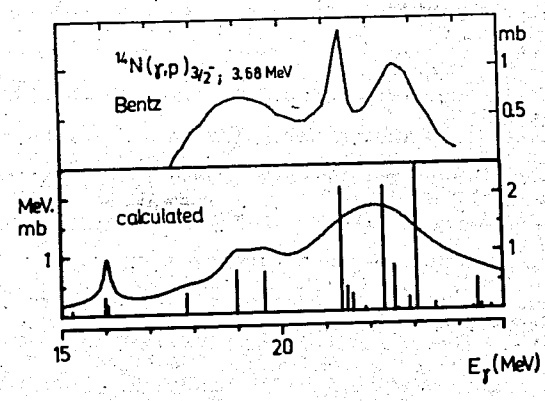


Fig. 6. Experimental and calculated $^{14}N(\gamma,p)_{3/2^-}$, 3.68 MeV cross-sections. The experimental data are taken from ref.[8].

sition involves l=3 transfer. Apart from $\gamma$-de-excitation, decay channels for this level would be opened by admixing $2\hbar\omega$ excitations in the low-lying states of $^{12}C$. Since no experimental data on the decay modes of this level are available we have included the corresponding strength into the secondary decay branch to the $^{12}C$ ground state.

Table 2 contains also the branches to several levels in $^{12}C$. The calculated relative yield to the ground state is in full agreement with the measured value[8]. As to the first $2^+$ state and the $\alpha$ - instable levels there is obvious disagreement with the data[8,12]. One should note, however, that the experiments were performed only up to 25 and 29 MeV, respectively, and we expect the high-energy tail to populate preferably excited states.

In the present paper we have not considered the energy spectra of outgoing particles as a function of their kinetic energy. These spectra are formed by a large number of partial transitions, including many secondary particles. Therefore the interpretation of such curves becomes difficult. On the other hand, the strong population of excited states of $^{13}N$ and $^{13}C$ (after primary nucleon emission) and also of the $2^+$ level in $^{12}C$ makes it attractive to study the photo reactions by coincidence measurements involving fixed nucleon or $\gamma$ energies. As such examples we mention

(i) the proton spectrum of the decay to the bound $3/2^-$ state of $^{13}C$ in coincidence with the de-excitation photons to the g.s. ($E_\gamma$ = 3.68 MeV),

(ii) the same for the unbound long-living $5/2^-$, 7.55 MeV state in $^{13}C$.



Fig. 7. Total $^{14}N(\gamma,n)$ cross-section from ref.[13] and this calculation. For comparison, the data for the ground-state transition (ref.[11]) is also indicated.

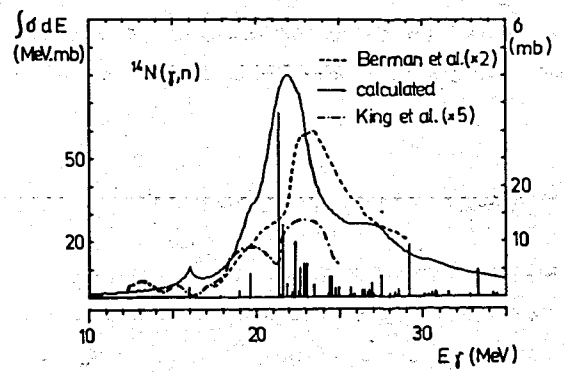


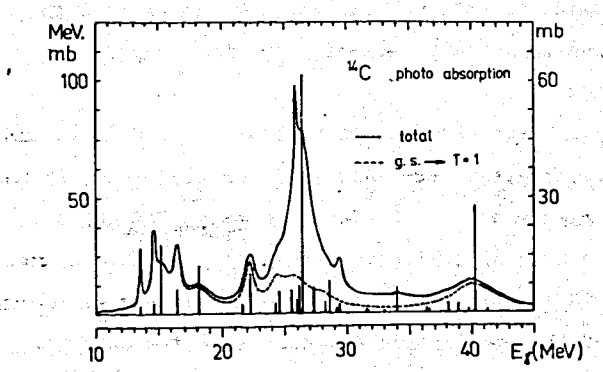


Fig. 8. Total photo absorption cross-section for $^{14}C$ nuclei.

(iii) the spectrum of primary protons in coincidence with the secondary neutrons of the decay of this long-lived level into $^{12}C$ ($E_n \simeq 2.5$ MeV).

These spectra must have resonance character and provide information about the detailed structure of the photo resonance.

## 3.2. The $^{14}C$ Photo Resonance

No experimental data on photo reactions on $^{14}C$ have been reported up till now. Nevertheless, we consider the analysis of this case as interesting. The isospin of the $^{14}C$ g.s. is $T_o=1$. Therefore one can study the isospin splitting of the giant resonance and the decay of its components. The $^{14}C$ photo absorption curve is clearly separated in three parts which can be assigned as:

(i) a pygmy resonance formed by levels $1^-$, $T=T_o$ around 15 MeV,

(ii) a usual giant resonance ($1^-$, $T=T_o+1$) around 25 MeV, and

(iii) a high-energy tail ($T=T_o$) above 40 MeV which is mainly due to 1s hole excitations (see fig.8). Also, a former calculation by Balashov et al.[18] yields a quite unusual energy distribution of the two isospin components of the absorption strength; the main maximum ($T=T_o+1$) was below the $T=T_o$ strength.

The $T=T_o+1$ part of the $^{14}C$ photo resonance decays to highly excited $T=3/2$ states in $^{13}C$. These states in turn decay by neutron emission. Hence, the dominating channel of the $^{14}C$ photo disintegration is the ($\gamma$, 2n) channel, and the total ($\gamma$,n) cross-section (see fig. 9a) shows the same structure as the ab-



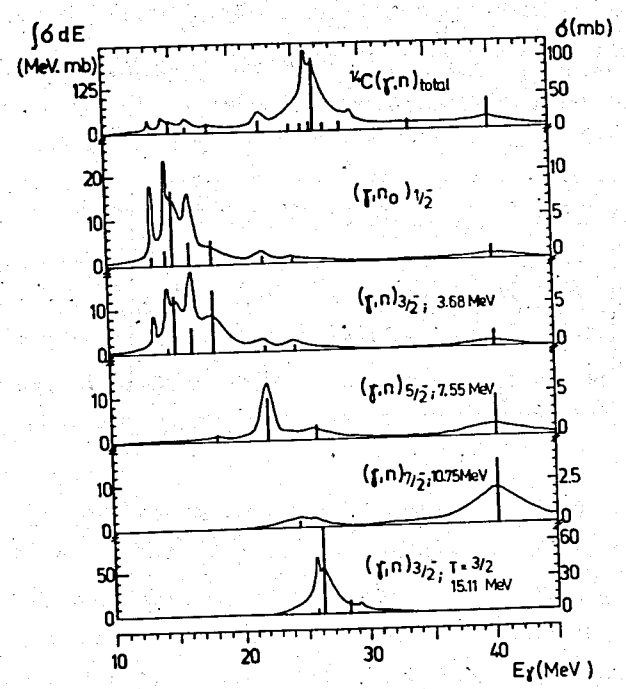


Fig. 9. Calculated cross-sections for the total and several partial ($\gamma$,n) reactions on $^{14}C$.

Table 4.

Branching ratios for the decay of the $^{14}C$ photo resonance. The relative values (in %) refer to the integral photo absorption cross-section

| | $^{13}C$ | | | | | | $^{12}C$ | | |
|---|---|---|---|---|---|---|---|---|---|
| final level | $1/2^-$ | $3/2^-$ | $5/2^-$ | $7/2^-$ | $3/2^-$ | T=3/2 | $0^+$ | $2^+$ | $\alpha$-in-stable |
| E(MeV) | g.s. | 3.68 | 7.55 | 10.75 | 15.11 | | g.s. | 4.44 | |
| branch (%) | 11.3 | 12.6 | 7.0 | 4.8 | 37.0 | | 4.3 | 17.0 | 6.6 |



sorption curve. The proton decay is negligible. As for the $^{14}N$ case, the yield of transitions to opposite-parity states in $^{13}C$ is small (about 5%), in contrast to the result of ref.[18].

Figure 9 summarizes also the partial ($\gamma$,n) cross-sections to the lowest $^{13}C$ levels which are strongly populated in the decay. The pygmy resonance decays to the g.s. and first excited $3/2^-$ state in $^{13}C$. The strong dipole state at 26 MeV decays only to the lowest $3/2^-$, T=3/2 level in $^{13}C$. This branch is not included in the secondary decay to $^{12}C$ since there is no T=1 level below this lowest T=3/2 one. A more complete description should include isospin mixing in parent and daughter nuclei and the $\gamma$-de-excitation of the T=3/2 level.

The high-energy part above 40 MeV of the photo resonance decays to excited levels of the residual nucleus above 10 MeV. However, in light nuclei at the upper end of the 1p shell the contribution of 1s hole excitations is not important. The decay properties of these states will be influenced by admixture of more complicated configurations as $2\hbar\omega$ and $3\hbar\omega$ excitations, respectively. As a result they will be spreaded over a wide energy region.

## Summary

We have investigated total and partial photonuclear cross-sections in the framework of the bound-state shell model combined with R matrix theory. The shell-model basis contains all non-spurious $1\hbar\omega$ excitations. A detailed comparison of the calculated cross-sections with data reported on the $^{14}N$ nucleus

demonstrates both applicability and drawbacks of our method. The model reproduces qualitatively the gross structure of the photo resonance and also the partial cross-sections of photonuclear reactions. Quantitative deviations arise because the model exhausts the dipole sum already in the energy region up to 30 MeV while in the experiment some part of the strength is shifted to higher photon energies. To account for this phenomenon, more refined calculations including higher excitations would be necessary (see e.g. Walker[19] ). For a deeper understanding of the giant resonance some additional experimental investigations of partial transitions are required. Of particular interest we consider the coincidence experiments mentioned above.

The study of the $^{14}C$ system showed that the photo disintegration of light nuclei with $T_o=0$ is characterized by isospin splitting of the photo resonance. The $T=T_o$ excitation creates the pygmy resonance which decays to low-lying $T=T_o-1/2$ levels of the daughter nuclei; only this part of the photo cross-section is seen in the inverse $(p,\gamma)$ reaction. The main maximum $(T=T_o+1)$ populates the $T=T_o+1/2$ levels in the residual nuclei above the nucleon threshold.

For the nuclei at the upper end of the 1p shell the yield of photo disintegration to the non-normal parity levels of the daughter nuclei is only about 5 percent, and the contribution of 1s hole excitations is unimportant.

We hope that this model will also apply to other 1p shell nuclei and also to other resonance features which are seen for instance in muon capture, electron scattering, etc.

We greatly acknowledge support by the Academy of Science and the Ministry of Science and Engineering, of the GDR and by the Joint Institute of Nuclear Research, Dubna in realizing this co-operation.



## References

1. H.U.Jäger, H.R.Kissener and R.A.Eramzhian, Nucl.Phys. A171 (1971) 16, 584.
2. S.Cohen and D.Kurath, Nucl.Phys. 73(1965) 1; A101 (1967) 1;
3. V.Gillet and E.A.Sanderson, Nucl.Phys. 88(1966) 363.
4. V.G.Neudachin and Yu.F.Smirnov, Atomic Energy Review 3 N° 3 (1965) 157.
5. L.R.B.Elton, Nuclear sizes. (Oxford University Press, 1961).
6. N.Bezíc, D.Brajnik, D.Jamnik and G.Kernel, Nucl.Phys. A128 (1969) 426.
7. H.G.Clerc and E.Kuphal, Z.Phys. 211 (1968) 452.
8. E.J.Bentz, Preprints, to be published in Phys.Rev.
9. I.Wahlström and B.Forkman, Arkiv for Fysik 18 (1960) 83.
10. R.Kosiek, K.Maier and K.Schlüpmann, Phys.Lett. 9 (1964) 260.
11. J.D.King, R.N.Haslam and R.W.Parsons, Can.J.Phys. 38(1960) 231.
12. M.N.Thompson, R.J.J.Stewart and J.E.M.Thompson, Phys.Lett. 31B (1970) 211.
13. B.L.Berman, S.C.Fultz, J.T.Galdwell, M.A.Kelly and S.S.Dietrich, Phys.Rev. C2 (1970) 2318.
14. A.P.Komar, Ya.Krzhemenek and I.P.Yavor, Nucl.Phys. 34(1962) 551.
15. A.I.Gorbunov, V.A.Dubrovina, V.A.Osipova, V.S.Silaeva and P.A.Cherenkov, J.Exp.Theor.Phys. 42 (1962) 747.
16. N.G.Goncharova, Jad.Fiz. 15 (1972) 242.
17. V.V.Balashov, D.Pal. and V.N.Fetisov, Phys.Lett., 17 (1965) 290.
18. V.V.Balashov, L.Mailing, L.A.Ramasanova, K.V.Shitikova and E.L.Yadrovskij, Izv.Akad.Nauk SSSR (ser.fiz.) 29(1965) 1177.

18. V.V.Balashov, L.Mailing, L.A.Ramasanova, K.V.Shitikova and E.L.Yadrovskij, Izv.Akad.Nauk SSSR (ser.fiz.) 29 (1965) 1177.

19. G.E.Walker, Phys.Rev. 174 (1968) 1290.

20. R.W.Gellie, K.H.Lokan, N.K.Sherman, R.G.Johnson and J.I.Lodge, Can.J.Phys. 50 (1972) 1689.

21. F.Riess, W.J.O'Connell and P.Paul, Nucl.Phys. A175(1971) 462.

Received by Publishing Department
on January 16, 1973.